Non-classical plate model for single-layered graphene sheet for axial buckling

Babak Safaei [1a], Farzad Hamed Khoda [2b] and A.M. Fattahi [*2]

[1] *Department of Mechanical Engineering, Tsinghua University, Beijing 100084, China*
[2] *Department of Mechanical Engineering, Tabriz Branch, Islamic Azad University, Tabriz, Iran*

Abstract.   In this work, the effect of size on the axial buckling behavior of single-layered graphene sheets embedded in elastic media is studied. We incorporate Eringen's nonlocal elasticity equations into three plate theories of first order shear deformation theory, higher order shear deformation theory, and classical plate theory. The surrounding elastic media are simulated using Pasternak and Winkler foundation models and their differences are evaluated. The results obtained from different nonlocal plate theories include the values of Winkler and Pasternak modulus parameters, mode numbers, nonlocal parameter, and side lengths of square SLGSs. We show here that axial buckling behavior strongly depends on modulus and nonlocal parameters, which have different values for different mode numbers and side lengths. In addition, we show that in different nonlocal plate theories, nonlocality is more influential in first order shear deformation theory, especially in certain range of nonlocal parameters.

1. Introduction

One can imagine a single-walled carbon nanotube (SWCNT) as a rolled two-dimensional single-layered graphene sheet (SLGS). Depending on the direction along which the graphene sheet is rolled, there are two types of armchair and zigzag carbon nanotubes (CNTs).

Prediction of the behaviors of nanostructures under different loads is performed using theoretical analyses. Kitipornchai, He and Liew (Kitipornchai *et al.* 2005) studied the vibration of multi layered graphene sheets (MLGSs) under simply supported boundary conditions with a continuum model based on classical plate theory (CLPT). Liew, He and Kitipornchai (Liew *et al.* 2006) investigated the vibration responses of MLSGs embedded in elastic matrices with a continuum model. Behfar and Naghdabadi (2005) investigated the nanoscale vibration of MLSGs embedded in elastic media. They assumed each MLSGs layer as an orthotropic plate with different elastic modulus in two perpendicular directions.

Peddieson, Buchanan and McNitt (Peddieson *et al.* 2003) used nonlocal elasticity for the evaluation of size effects on micro- and nanoscale structures. They investigated the bending of micro- and nano-beams with nonlocal elasticity and suggested that size had significant effect on nano-structures and the amounts of these effects depended on the values of nonlocal parameters. Nonlocal continuum model has attracted researchers due to its simplicity and efficiency in analyzing the behavior of

different nanostructures (Shen 2010, Sahmani and Fattahi 2017, Filiz and Aydogdu 2010, Shen *et al.* 2010, Safaei and Fattahi 2017, Yang *et al.* 2010, Hao *et al.* 2010, Alizadeh and Fattahi 2019, Kiani 2010, Zenkour 2018). Fattahi and Sahmani (2017) studied the postbuckling behavior of nanoshells reinforced with FG-CNTs under hydrostatic pressures.

In polymer nanocomposites, like many other nano-scaled compounds, nanostructures can be embedded in elastic surroundings. Generally, these elastic media are simulated with Winkler foundation model (Fattahi and Sahmani 2017). However, this model cannot take into account the continuity of media. Elastic foundation can be more practically modeled with Pasternak foundation model (Winkler 1867, Pasternak 1954) in which both transverse shear stress and normal pressure are considered by introducing two modulus parameters corresponding to each factor. Liew *et al.* (2006) employed Pasternak foundation model. The interaction of elastic media with graphene sheets were simulated by Pradhan and Murmu (2010) who achieved good results and verified the correctness of foundation modeling. In another work, Azizi *et al.* (2015) investigated the nonlinear free vibration characteristics of embedded nanobeams. Dynamic analysis of straight and wavy CNT/ polymer composite plates was carried out by Moradi-Dastjerdi and Momeni-Khabisi (2016) based on mesh free method.

Researchers have studied the effects of size on the mechanical behaviors of materials according to first-order shear deformation theory (FSDT) (Jalali *et al.* 2018) and nonlocal elasticity (Shahriari *et al.* 2018, Mohammadsalehi *et al.* 2017) theories. Free vibration (Moradi-Dastjerdi *et al.* 2017), biaxial buckling (Moradi-Dastjerdi *et al.* 2017), thermoelastic dynamic (Safaei *et al.* 2019) behaviors of sandwich plates with aggregated CNTs-reinforced nancomposite face sheets on elastic foundations have been

---

∗Corresponding author, Ph.D.,
 E-mail: a.fattahi@iaut.ac.ir
[a] Ph.D.
[b] MA

investigated with different plate theories.

Bouadi *et al*. (2018) developed a new nonlocal higher order shear deformation theory (HSDT) for buckling properties of single graphene sheet. Ebrahimi and Barati (2018) showed that temperature change, thermal loading type, surface effect, nonlocal parameter, boundary conditions and plate thickness significantly affected the buckling loads of flexoelectric nanoplates. Daouadji and Adim (2017) compared numerical results with 3D exact, quasi-3-dimensional and other HSDT solutions. Qin *et al*. (2019) by using FSDT investigated free vibration of rotating functionally graded CNT reinforced composite cylindrical shells with arbitrary boundary conditions. Moheimani and Ahmadian (2012) and Pasharavesh *et al*. (2011) employed nonlocal continuum theory to analytically evaluate the dynamic behavior and nonlinear vibration of nano-beams. Their results showed that nonlocal size effect potentially played a critical role in the structural analysis of nano-scaled dynamic and vibration behaviors of beams. Safaei *et al*. (2016) investigated the critical axial buckling strain of CNTs with different chiral angles. Fattahi and Safaei (2017) showed that higher CNTs volume fractions increased the stiffness of nanocomposite beams, especially with long-SWCNT reinforcements.

The investigation of the behavior and elastic properties of graphene plates and graphene-reinforced sheets is among the goals of this research. The innovation of this research and its difference with other research works is the application of Eringen's nonlocal theory in three plate theories as well as using Fourier's method for solving equations and comparing the three obtained modified theories for nanoscaled structures. Here, we consider size effect on the axial buckling behaviors of embedded SLGSs through the incorporation of Eringen's nonlocal elasticity equations (Eringen 1972) into different plate theories and introduce equations for critical axial buckling loads for each nonlocal plate theory. Then, different numerical results are presented to verify the effects of the values of length, mode number and nonlocal parameter in both Pasternak and Winkler foundation models.

2. Overview of different plate theories

A uniform square nanoplate with side length L and thickness h is assumed as shown in Fig. 1. Coordinate system (x, y, z) is introduced at one corner of nanoplate midplane such that x, y and z axes are assumed to be along the length, width and depth (thickness) directions of the nanoplate, respectively.

Displacement components (u_1, u_2, u_3) along corresponding axes (x, y, z) can be expressed in a general form as (Safaei and Fattahi 2017)

$$u_1 = -z\frac{\partial w}{\partial x} + \psi(z)\left(\frac{\partial w}{\partial x} + \varphi_x\right)$$
$$u_2 = -z\frac{\partial w}{\partial y} + \psi(z)\left(\frac{\partial w}{\partial y} + \varphi_y\right) \quad (1)$$
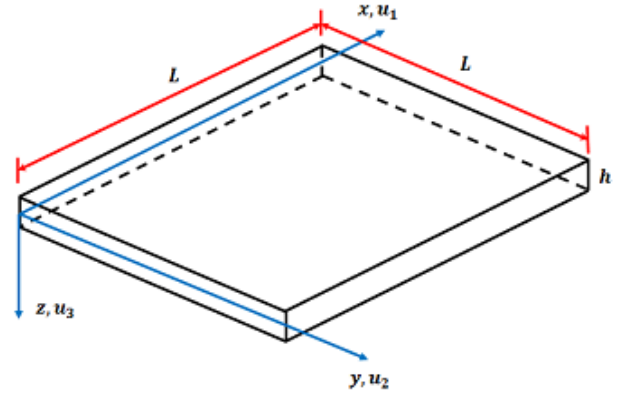$$u_3 = w(x,t)$$

Fig. 1 Schematic diagram of a nanoplate
(Safaei and Fattahi 2017)

where w is transverse displacement and φ_x and φ_y are angular displacements along x and y directions, respectively; $\psi(z)$ is shape function. For CLPT, FSDT and HSDT we have $\psi(Z) = 0$, $\psi(z) = z$, and $\psi(z) = z - \frac{4z^3}{3h^2}$, respectively.

2.1 Classical Plate Theory (CLPT)

Based on Eq. (1), strain-displacement relations suitable for CLPT can be given as

$$\varepsilon_{xx} = \frac{\partial u_1}{\partial x} = -z\frac{\partial^2 w}{\partial x^2} \quad (2a)$$

$$\varepsilon_{yy} = \frac{\partial u_2}{\partial y} = -z\frac{\partial^2 w}{\partial y^2} \quad (2b)$$

$$\gamma_{xy} = \frac{\partial u_1}{\partial y} + \frac{\partial u_2}{\partial x} = -2z\frac{\partial^2 w}{\partial x \partial y} \quad (2c)$$

$$\gamma_{xz} = \gamma_{yz} = 0 \quad (2d)$$

According to the principle of virtual displacement, the following equilibrium equation can be obtained for CLPT

$$\frac{\partial^2 M_{xx}}{\partial x^2} + \frac{\partial^2 M_{yy}}{\partial y^2} + 2\frac{\partial^2 M_{xy}}{\partial x \partial y} - P\left(\frac{\partial^2 w}{\partial x^2} + \frac{\partial^2 w}{\partial y^2}\right) = 0 \quad (3)$$

where P is critical axial buckling load and M is torque vector which can be calculated as

$$M = \{M_{xx}, M_{yy}, M_{xy}\}^T = \int_{-h/2}^{h/2}\{\sigma_{xx}, \sigma_{yy}, \sigma_{xy}\}^T z.dz \quad (4a)$$

$$M_{xx} = -D\left(\frac{\partial^2 w}{\partial x^2} + v\frac{\partial^2 w}{\partial y^2}\right)$$
$$M_{yy} = -D\left(\frac{\partial^2 w}{\partial y^2} + v\frac{\partial^2 w}{\partial x^2}\right) \quad (4b)$$

$$M_{xy} = -D(1-v)(\frac{\partial^2 w}{\partial x \partial y}) \tag{4c}$$

$$D = \frac{Eh^3}{12(1-v^2)} \tag{4d}$$

Eq. (3) can be written in terms of displacements as

$$-\frac{Eh^3}{12(1-v^2)}\left(\frac{\partial^4 w}{\partial x^4} + 2v\frac{\partial^4 w}{\partial x^2 \partial y^2} + \frac{\partial^4 w}{\partial y^4}\right)$$
$$-\frac{Eh^3}{6(1+v)}\frac{\partial^4 w}{\partial x^2 \partial y^2} - P\left(\frac{\partial^2 w}{\partial x^2} + \frac{\partial^2 w}{\partial y^2}\right) = 0 \tag{5}$$

2.2 First Order Shear Deformation Theory (FSDT)

FSDT takes into account the effects of rotational inertia and shear deformation and therefore, the straight lines vertical to the mid-plane of the plate disappear. However, it was assumed that transverse shear stress had linear distribution along plate thickness. The following strain-displacement relations can be expressed based on Eq. (1) as

$$\varepsilon_{xx} = \frac{\partial u_1}{\partial x} = z\frac{\partial \varphi_x}{\partial x} \tag{6a}$$

$$\varepsilon_{yy} = \frac{\partial u_2}{\partial y} = z\frac{\partial \varphi_y}{\partial y} \tag{6b}$$

$$\gamma_{xy} = \frac{\partial u_1}{\partial y} + \frac{\partial u_2}{\partial x} = z(\frac{\partial \varphi_x}{\partial y} + \frac{\partial \varphi_y}{\partial x}) \tag{6c}$$

$$\gamma_{xz} = \frac{\partial u_1}{\partial z} + \frac{\partial u_3}{\partial x} = \frac{\partial w}{\partial x} + \varphi_x \tag{6d}$$

$$\gamma_{yz} = \frac{\partial u_2}{\partial z} + \frac{\partial u_3}{\partial y} = \frac{\partial w}{\partial y} + \varphi_y \tag{6e}$$

Based on virtual displacement principle, the following equilibrium equations are obtained for FSDT

$$\frac{\partial Q_{xx}}{\partial x} + \frac{\partial Q_{yy}}{\partial y} - P(\frac{\partial^2 w}{\partial x^2} + \frac{\partial^2 w}{\partial y^2}) = 0 \tag{7a}$$

$$\frac{\partial M_{xx}}{\partial x} + \frac{\partial M_{xy}}{\partial y} - Q_{xx} = 0 \tag{7b}$$

$$\frac{\partial M_{yy}}{\partial y} + \frac{\partial M_{xy}}{\partial x} - Q_{yy} = 0 \tag{7c}$$

$$\{Q_x, Q_y\}^T = \kappa \int_{-h/2}^{h/2} \{\sigma_{yz}, \sigma_{xz}\}^T dz \tag{7d}$$

where Q is shear force per unit length and κ is shear correction coefficient. Eq. (7) can be written in terms of displacements as

$$\kappa Gh\left(\frac{\partial \varphi_x}{\partial x} + \frac{\partial \varphi_y}{\partial y} + \frac{\partial^2 w}{\partial x^2} + \frac{\partial^2 w}{\partial y^2}\right)$$
$$-P(\frac{\partial^2 w}{\partial x^2} + \frac{\partial^2 w}{\partial y^2}) = 0 \tag{8a}$$

$$\frac{Eh^3}{(1-v^2)}\left(\frac{\partial^2 \varphi_x}{\partial x^2} + v\frac{\partial^2 \varphi_y}{\partial x \partial y}\right)$$
$$+\frac{Eh^3}{24(1+v)}\left(\frac{\partial^2 \varphi_y}{\partial x \partial y} + \frac{\partial^2 \varphi_x}{\partial y^2}\right) - \kappa Gh\left(\varphi_x + \frac{\partial w}{\partial x}\right) = 0 \tag{8b}$$

$$\frac{Eh^3}{12(1-v^2)}\left(\frac{\partial^2 \varphi_y}{\partial y^2} + v\frac{\partial^2 \varphi_x}{\partial x \partial y}\right)$$
$$+\frac{Eh^3}{24(1+v)}\left(\frac{\partial^2 \varphi_y}{\partial x^2} + \frac{\partial^2 \varphi_x}{\partial x \partial y}\right) - \kappa Gh\left(\varphi_y + \frac{\partial w}{\partial y}\right) = 0 \tag{8c}$$

2.3 Higher Order Shear Deformation Theory (HSDT)

In third-order shear deformation theory, transverse shear stress has a parabolic distribution along the thickness of the plate with no shear correction factor to satisfy transverse shear stress conditions on the lower and upper layers of plate cross-section. Strain-displacement relations for HSDT can be written according to Eq. (1) as

$$\varepsilon_{xx} = \frac{\partial u_1}{\partial x} = z\frac{\partial \varphi_x}{\partial x} - \frac{4z^3}{3h^2}\left(\frac{\partial \varphi_x}{\partial x} + \frac{\partial^2 w}{\partial x^2}\right) \tag{9a}$$

$$\varepsilon_{yy} = \frac{\partial u_2}{\partial y} = z\frac{\partial \varphi_y}{\partial y} - \frac{4z^3}{3h^2}\left(\frac{\partial \varphi_y}{\partial y} + \frac{\partial^2 w}{\partial y^2}\right) \tag{9b}$$

$$\gamma_{xy} = \frac{\partial u_1}{\partial y} + \frac{\partial u_2}{\partial x} = z\left(\frac{\partial \varphi_x}{\partial y} + \frac{\partial \varphi_y}{\partial x}\right)$$
$$-\frac{4z^3}{3h^2}\left(\frac{\partial \varphi_x}{\partial y} + \frac{\partial \varphi_y}{\partial x} + 2\frac{\partial^2 w}{\partial x \partial y}\right) \tag{9c}$$

$$\gamma_{xz} = \frac{\partial u_1}{\partial z} + \frac{\partial u_3}{\partial x} = \left(1 - \frac{4z^2}{h^2}\right)\left(\frac{\partial w}{\partial x} + \varphi_x\right) \tag{9d}$$

$$\gamma_{yz} = \frac{\partial u_2}{\partial z} + \frac{\partial u_3}{\partial y} = \left(1 - \frac{4z^2}{h^2}\right)\left(\frac{\partial w}{\partial y} + \varphi_y\right) \tag{9e}$$

According to the principle of virtual displacement, equilibrium equations can be obtained for HSDT as

$$\frac{\partial Q_{xx}}{\partial x} + \frac{\partial Q_{yy}}{\partial y} - \frac{4}{h^2}\left(\frac{\partial S_{xx}}{\partial x} + \frac{\partial S_{yy}}{\partial y}\right)$$
$$+\frac{4}{3h^2}\left(\frac{\partial^2 R_{xx}}{\partial x^2} + \frac{\partial^2 R_{yy}}{\partial y^2} + 2\frac{\partial^2 R}{\partial x \partial y}\right)$$
$$-P(\frac{\partial^2 W}{\partial x^2} + \frac{\partial^2 W}{\partial y^2}) = 0 \tag{10a}$$

$$\frac{\partial M_{xx}}{\partial x} + \frac{\partial M_{xy}}{\partial y} - \frac{4}{3h^2}\left(\frac{\partial R_{xx}}{\partial x} + \frac{\partial R_{xy}}{\partial y}\right)$$

$$-Q_{xx} + \frac{4}{h^2}S_{xx} = 0 \tag{10b}$$

$$\frac{\partial M_{yy}}{\partial y} + \frac{\partial M_{xy}}{\partial x} - \frac{4}{3h^2}\left(\frac{\partial R_{yy}}{\partial y} + \frac{\partial R_{xy}}{\partial x}\right)$$

$$-Q_{yy} + \frac{4}{h^2}S_{yy} = 0 \tag{10c}$$

Where

$$R = \{R_{xx}, R_{yy}, R_{xy}\}^T = \int_{-h/2}^{h/2} Z^3\{\sigma_{xx}, \sigma_{yy}, \sigma_{xy}\}^T dz \tag{10d}$$

And

$$S = \{S_{xx}, S_{yy}\}^T = \int_{-h/2}^{h/2} Z^2\{\sigma_{xz}, \sigma_{yz}\}^T dz \tag{10e}$$

The governing equations presented in Eq. (10) can be expressed in terms of displacements as

$$\frac{8Gh}{15}\left(\frac{\partial \varphi_x}{\partial x} + \frac{\partial \varphi_y}{\partial y} + \frac{\partial^2 w}{\partial x^2} + \frac{\partial^2 w}{\partial y^2}\right)$$
$$+\frac{4Eh^3}{315(1-v^2)}\left[\frac{\partial^3 \varphi_x}{\partial x^3} + \frac{\partial^3 \varphi_y}{\partial y^3}\right.$$
$$\left.+v\left(\frac{\partial^3 \varphi_x}{\partial x \partial y^2} + \frac{\partial^3 \varphi_y}{\partial x^2 \partial y}\right)\right]$$
$$-\frac{4Eh^3}{252(1-v^2)}\left(\frac{\partial^4 w}{\partial x^4} + \frac{\partial^4 w}{\partial y^4} + 2v\frac{\partial^4 w}{\partial x^2 \partial y^2}\right) \tag{11a}$$
$$+\frac{4Eh^3}{315(1+v)}\left(\frac{\partial^3 \varphi_y}{\partial x^2 \partial y} + \frac{\partial^3 \varphi_x}{\partial x \partial y^2}\right)$$
$$-\frac{Eh^3}{126(1+v)}\frac{\partial^4 w}{\partial x^2 \partial y^2} - P\left(\frac{\partial^2 w}{\partial x^2} + \frac{\partial^2 W}{\partial y^2}\right) = 0$$

$$\frac{17Eh^3}{315(1-v^2)}\left(\frac{\partial^2 \varphi_x}{\partial x^2} + v\frac{\partial^2 \varphi_y}{\partial x \partial y}\right)$$
$$-\frac{4Eh^3}{315(1-v^2)}\left(\frac{\partial^3 w}{\partial x^3} + v\frac{\partial^3 w}{\partial x \partial y^2}\right)$$
$$+\frac{17Eh^3}{630(1+v)}\left(\frac{\partial^2 \varphi_y}{\partial x \partial y} + \frac{\partial^2 \varphi_x}{\partial y^2}\right) - \frac{4Eh^3}{315(1+v)}\frac{\partial^3 w}{\partial x \partial y^2} \tag{11b}$$
$$-\frac{8Gh}{15}\left(\varphi_x + \frac{\partial w}{\partial x}\right) = 0$$

$$\frac{17Eh^3}{315(1-v^2)}\left(\frac{\partial^2 \varphi_y}{\partial y^2} + v\frac{\partial^2 \varphi_x}{\partial x \partial y}\right)$$
$$-\frac{4Eh^3}{315(1-v^2)}\left(\frac{\partial^3 w}{\partial y^3} + v\frac{\partial^3 w}{\partial y \partial x^2}\right)$$
$$+\frac{17Eh^3}{630(1+v)}\left(\frac{\partial^2 \varphi_y}{\partial x^2} + \frac{\partial^2 \varphi_x}{\partial x \partial y}\right) \tag{11c}$$
$$-\frac{4Eh^3}{315(1+v)}\frac{\partial^3 w}{\partial y \partial x^2} - \frac{8Gh}{15}\left(\varphi_y + \frac{\partial w}{\partial y}\right) = 0$$
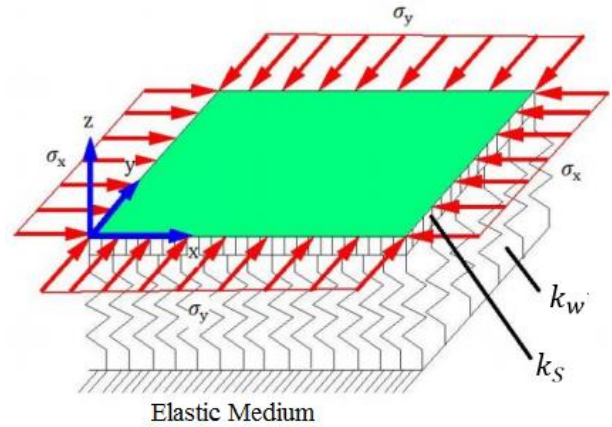

Fig. 2 Geometric schematic diagram of rectangular plate subjected to axial loads embedded in elastic medium modeled with Pasternak foundation model

3. Nonlocal plate theories for axial buckling of SLGSs

Eringen (1972) was the first person to introduce nonlocal elasticity theory. For isotropic and homogenous elastic continuum, linear nonlocal elasticity theory can be written as

$$(1 - \mu \nabla^2)\sigma_{kl,l}(x) = \sigma_{kl}(x) \tag{12}$$

where μ is nonlocal or small scale parameter appropriate to material and internal characteristic constant and $\triangledown$ is Laplacian operator. The value of non-local parameter is not constant and depends on the nature of motion, number of modes, supporting conditions, and the number of walls and layers and so far, there have been only a few reports on its exact value. Available data shows that the acceptable range for non-local parameter is 0 to 4 nm (Peddieson *et al.* 2003) and therefore, we use this interval for this parameter in this study.

Elastic medium surrounded the SLGSs investigated in this work. Pasternak foundation model (Pasternak 1954) (Fig. 2) is used to simulate elastic surrounding. The loading of this foundation model is expressed as

$$Q_{pasternak} = k_w w - k_S\left(\frac{\partial^2 w}{\partial x^2} + \frac{\partial^2 w}{\partial y^2}\right) \tag{13}$$

where k_w is Winkler modulus parameter corresponding to normal pressure and k_S is Pasternak modulus parameter relevant to transverse shear stress. Neglecting shear deformation effects ($k_S = 0$) reduces the foundation model to Winkler model (Winkler 1867).

3.1 Classical Plate Theory (CLPT)

By the addition of the terms of elastic medium to the governing equation of CLPT, we find

$$-\frac{Eh^3}{12(1-v^2)}\left(\frac{\partial^4 w}{\partial x^4} + 2v\frac{\partial^4 w}{\partial x^2 \partial y^2} + \frac{\partial^4 w}{\partial y^4}\right) \tag{14}$$

$$-\frac{Eh^3}{6(1+v)}\frac{\partial^4 w}{\partial x^2 \partial y^2} - P\left(\frac{\partial^2 w}{\partial x^2} + \frac{\partial^2 W}{\partial y^2}\right) - k_w w$$

$$+k_S\left(\frac{\partial^2 w}{\partial x^2} + \frac{\partial^2 w}{\partial y^2}\right) = 0$$

According to Eq. (12), the only constitutive relation for nonlocal CLPT model with elastic medium is obtained as

$$-\frac{Eh^3}{12(1-v^2)}\left(\frac{\partial^4 w}{\partial x^4} + 2v\frac{\partial^4 w}{\partial x^2 \partial y^2} + \frac{\partial^4 w}{\partial y^4}\right)$$

$$-\frac{Eh^3}{6(1+v)}\frac{\partial^4 w}{\partial x^2 \partial y^2} - P\left(\frac{\partial^2 w}{\partial x^2} + \frac{\partial^2 W}{\partial y^2}\right)$$

$$+\mu P\left(\frac{\partial^4 w}{\partial x^4} + 2\frac{\partial^4 w}{\partial x^2 \partial y^2} + \frac{\partial^4 W}{\partial y^4}\right) - k_w w \qquad (15)$$

$$+k_S\left(\frac{\partial^2 w}{\partial x^2} + \frac{\partial^2 w}{\partial y^2}\right) + \mu k_w\left(\frac{\partial^2 w}{\partial x^2} + \frac{\partial^2 w}{\partial y^2}\right)$$

$$-\mu k_S\left(\frac{\partial^4 w}{\partial x^4} + 2\frac{\partial^4 w}{\partial x^2 \partial y^2} + \frac{\partial^4 w}{\partial y^4}\right) = 0$$

3.2 First Order Shear Deformation Theory (FSDT)

Introducing elastic medium terms into governing equations of FSDT gives

$$kGh\left(\frac{\partial \varphi_x}{\partial x} + \frac{\partial \varphi_y}{\partial y} + \frac{\partial^2 w}{\partial x^2} + \frac{\partial^2 w}{\partial y^2}\right) - P\left(\frac{\partial^2 w}{\partial x^2} + \frac{\partial^2 w}{\partial y^2}\right)$$

$$-k_w w + k_S\left(\frac{\partial^2 w}{\partial x^2} + \frac{\partial^2 w}{\partial y^2}\right) = 0 \qquad (16a)$$

$$\frac{Eh^3}{12(1-v^2)}\left(\frac{\partial^2 \varphi_x}{\partial x^2} + v\frac{\partial^2 \varphi_y}{\partial x \partial y}\right)$$

$$+\frac{Eh^3}{24(1+v)}\left(\frac{\partial^2 \varphi_y}{\partial x \partial y} + \frac{\partial^2 \varphi_x}{\partial y^2}\right) - \kappa Gh\left(\varphi_x + \frac{\partial w}{\partial x}\right) = 0 \qquad (16b)$$

$$\frac{Eh^3}{12(1-v^2)}\left(\frac{\partial^2 \varphi_y}{\partial y^2} + v\frac{\partial^2 \varphi_x}{\partial x \partial y}\right)$$

$$+\frac{Eh^3}{24(1+v)}\left(\frac{\partial^2 \varphi_y}{\partial x^2} + \frac{\partial^2 \varphi_x}{\partial x \partial y}\right) - \kappa Gh\left(\varphi_y + \frac{\partial w}{\partial y}\right) = 0 \qquad (16c)$$

Based on Eq. (12), constitutive relations for nonlocal FSDT model with elastic medium are obtained as

$$\kappa Gh\left(\frac{\partial \varphi_x}{\partial x} + \frac{\partial \varphi_y}{\partial y} + \frac{\partial^2 w}{\partial x^2} + \frac{\partial^2 w}{\partial y^2}\right) - P\left(\frac{\partial^2 w}{\partial x^2} + \frac{\partial^2 w}{\partial y^2}\right)$$

$$+\mu P\left(\frac{\partial^4 w}{\partial x^4} + 2\frac{\partial^4 w}{\partial x^2 \partial y^2} + \frac{\partial^4 W}{\partial y^4}\right) - k_w w$$

$$+k_S\left(\frac{\partial^2 w}{\partial x^2} + \frac{\partial^2 w}{\partial y^2}\right) + \mu k_w\left(\frac{\partial^2 w}{\partial x^2} + \frac{\partial^2 w}{\partial y^2}\right) \qquad (17a)$$

$$-\mu k_S\left(\frac{\partial^4 w}{\partial x^4} + 2\frac{\partial^4 w}{\partial x^2 \partial y^2} + \frac{\partial^4 w}{\partial y^4}\right) = 0$$

$$\frac{Eh^3}{12(1-v^2)}\left(\frac{\partial^2 \varphi_x}{\partial x^2} + v\frac{\partial^2 \varphi_y}{\partial x \partial y}\right)$$

$$+\frac{Eh^3}{24(1+v)}\left(\frac{\partial^2 \varphi_y}{\partial x \partial y} + \frac{\partial^2 \varphi_x}{\partial y^2}\right) - \kappa Gh\left(\varphi_x + \frac{\partial w}{\partial x}\right) = 0 \qquad (17b)$$

$$\frac{Eh^3}{12(1-v^2)}\left(\frac{\partial^2 \varphi_y}{\partial y^2} + v\frac{\partial^2 \varphi_x}{\partial x \partial y}\right)$$

$$+\frac{Eh^3}{24(1+v)}\left(\frac{\partial^2 \varphi_y}{\partial x^2} + \frac{\partial^2 \varphi_x}{\partial x \partial y}\right) - \kappa Gh\left(\varphi_y + \frac{\partial w}{\partial y}\right) = 0 \qquad (17c)$$

3.3 Higher Order Shear Deformation Theory (HSDT)

Introducing elastic medium terms into the governing equations of HSDT gives

$$\frac{8Gh}{15}\left(\frac{\partial \varphi_x}{\partial x} + \frac{\partial \varphi_y}{\partial y} + \frac{\partial^2 w}{\partial x^2} + \frac{\partial^2 w}{\partial y^2}\right)$$

$$+\frac{4Eh^3}{315(1-v^2)}\left[\frac{\partial^3 \varphi_x}{\partial x^3} + \frac{\partial^3 \varphi_y}{\partial y^3}\right.$$

$$+v\left(\frac{\partial^3 \varphi_x}{\partial x \partial y^2} + \frac{\partial^3 \varphi_y}{\partial x^2 \partial y}\right)\Bigg]$$

$$-\frac{4Eh^3}{252(1-v^2)}\left(\frac{\partial^4 w}{\partial x^4} + \frac{\partial^4 w}{\partial y^4} + 2v\frac{\partial^4 w}{\partial x^2 \partial y^2}\right) \qquad (18a)$$

$$+\frac{4Eh^3}{315(1+v)}\left(\frac{\partial^3 \varphi_y}{\partial x^2 \partial y} + \frac{\partial^3 \varphi_x}{\partial x \partial y^2}\right)$$

$$-\frac{Eh^3}{126(1+v)}\frac{\partial^4 w}{\partial x^2 \partial y^2} - P\left(\frac{\partial^2 w}{\partial x^2} + \frac{\partial^2 w}{\partial y^2}\right)$$

$$-k_w w + k_S\left(\frac{\partial^2 w}{\partial x^2} + \frac{\partial^2 w}{\partial y^2}\right) = 0$$

$$\frac{17Eh^3}{315(1-v^2)}\left(\frac{\partial^2 \varphi_x}{\partial x^2} + v\frac{\partial^2 \varphi_y}{\partial x \partial y}\right)$$

$$-\frac{4Eh^3}{315(1-v^2)}\left(\frac{\partial^3 w}{\partial x^3} + v\frac{\partial^3 w}{\partial x \partial y^2}\right)$$

$$+\frac{17Eh^3}{630(1+v)}\left(\frac{\partial^2 \varphi_y}{\partial x \partial y} + \frac{\partial^2 \varphi_x}{\partial y^2}\right) \qquad (18b)$$

$$-\frac{4Eh^3}{315(1+v)}\frac{\partial^3 w}{\partial x \partial y^2} - \frac{8Gh}{15}\left(\varphi_x + \frac{\partial w}{\partial x}\right) = 0$$

$$\frac{17Eh^3}{315(1-v^2)}\left(\frac{\partial^2 \varphi_y}{\partial y^2} + v\frac{\partial^2 \varphi_x}{\partial x \partial y}\right)$$

$$-\frac{4Eh^3}{315(1-v^2)}\left(\frac{\partial^3 w}{\partial y^3} + v\frac{\partial^3 w}{\partial y \partial x^2}\right)$$

$$+\frac{17Eh^3}{630(1+v)}\left(\frac{\partial^2 \varphi_y}{\partial x^2} + \frac{\partial^2 \varphi_x}{\partial x \partial y}\right) \qquad (18c)$$

$$-\frac{4Eh^3}{315(1+v)}\frac{\partial^3 w}{\partial y \partial x^2} - \frac{8Gh}{15}\left(\varphi_y + \frac{\partial w}{\partial y}\right) = 0$$

According to Eq. (13), constitutive relations for nonlocal HSDT model with elastic medium are obtained as

$$\frac{8Gh}{15}\left(\frac{\partial \varphi_x}{\partial x} + \frac{\partial \varphi_y}{\partial y} + \frac{\partial^2 w}{\partial x^2} + \frac{\partial^2 w}{\partial y^2}\right) \tag{19a}$$

$$+\frac{4Eh^3}{315(1-v^2)}\left[\frac{\partial^3 \varphi_x}{\partial x^3} + \frac{\partial^3 \varphi_y}{\partial y^3}\right.$$
$$+v\left(\frac{\partial^3 \varphi_x}{\partial x \partial y^2} + \frac{\partial^3 \varphi_y}{\partial x^2 \partial y}\right)\right]$$
$$-\frac{4Eh^3}{252(1-v^2)}\left(\frac{\partial^4 w}{\partial x^4} + \frac{\partial^4 w}{\partial y^4} + 2v\frac{\partial^4 w}{\partial x^2 \partial y^2}\right)$$
$$+\frac{4Eh^3}{315(1+v)}\left(\frac{\partial^3 \varphi_y}{\partial x^2 \partial y} + \frac{\partial^3 \varphi_x}{\partial x \partial y^2}\right)$$
$$-\frac{Eh^3}{126(1+v)}\frac{\partial^4 w}{\partial x^2 \partial y^2} - P\left(\frac{\partial^2 w}{\partial x^2} + \frac{\partial^2 w}{\partial y^2}\right) \tag{19a}$$
$$+\mu P\left(\frac{\partial^4 w}{\partial x^4} + \frac{\partial^4 w}{\partial x^2 \partial y^2}\right) - k_w w$$
$$+k_S\left(\frac{\partial^2 w}{\partial x^2} + \frac{\partial^2 w}{\partial y^2}\right) + \mu k_w\left(\frac{\partial^2 w}{\partial x^2} + \frac{\partial^2 w}{\partial y^2}\right)$$
$$-\mu k_S\left(\frac{\partial^4 w}{\partial x^4} + 2\frac{\partial^4 w}{\partial x^2 \partial y^2} + \frac{\partial^4 w}{\partial y^4}\right) = 0$$

$$\frac{17Eh^3}{315(1-v^2)}\left(\frac{\partial^2 \varphi_x}{\partial x^2} + v\frac{\partial^2 \varphi_y}{\partial x \partial y}\right)$$
$$-\frac{4Eh^3}{315(1-v^2)}\left(\frac{\partial^3 w}{\partial x^3} + v\frac{\partial^3 w}{\partial x \partial y^2}\right)$$
$$+\frac{17Eh^3}{630(1+v)}\left(\frac{\partial^2 \varphi_y}{\partial x \partial y} + \frac{\partial^2 \varphi_x}{\partial y^2}\right) \tag{19b}$$
$$-\frac{4Eh^3}{315(1+v)}\frac{\partial^3 w}{\partial x \partial y^2} - \frac{8Gh}{15}\left(\varphi_x + \frac{\partial w}{\partial x}\right) = 0$$

$$\frac{17Eh^3}{315(1-v^2)}\left(\frac{\partial^2 \varphi_y}{\partial y^2} + v\frac{\partial^2 \varphi_x}{\partial x \partial y}\right)$$
$$-\frac{4Eh^3}{315(1-v^2)}\left(\frac{\partial^3 w}{\partial y^3} + v\frac{\partial^3 w}{\partial y \partial x^2}\right)$$
$$+\frac{17Eh^3}{630(1+v)}\left(\frac{\partial^2 \varphi_y}{\partial x^2} + \frac{\partial^2 \varphi_x}{\partial x \partial y}\right) \tag{19c}$$
$$-\frac{4Eh^3}{315(1+v)}\frac{\partial^3 w}{\partial y \partial x^2} - \frac{8Gh}{15}\left(\varphi_y + \frac{\partial w}{\partial y}\right) = 0$$

4. Analytical solution for simply supported SLGSs

4.1 Exact solutions for critical axial buckling load

Exact solutions are provided to achieve critical axial buckling loads for each nonlocal theory for SLGSs in elastic media. Simply supported boundary conditions can be expressed as

At $x = 0$ and $x = L$

$$w = 0, \quad \varphi_y = 0, \quad M_{xx} = 0 \tag{20a}$$

At $y = 0$ and $y = L$

$$w = 0, \quad \varphi_x = 0, \quad M_{yy} = 0 \tag{20b}$$

Angular and transverse displacements are assumed in the following general form to satisfy boundary conditions

$$w(x,y) = \sum_{m=1}^{\infty}\sum_{n=1}^{\infty} W_{mn} \sin\left(\frac{m\pi x}{L}\right)\sin\left(\frac{n\pi y}{L}\right) \tag{21a}$$

$$\varphi_x(x,y) = \sum_{m=1}^{\infty}\sum_{n=1}^{\infty} A_{mn} \cos\left(\frac{m\pi x}{L}\right)\sin\left(\frac{n\pi y}{L}\right) \tag{21b}$$

$$\varphi_y(x,y) = \sum_{m=1}^{\infty}\sum_{n=1}^{\infty} B_{mn} \sin\left(\frac{m\pi x}{L}\right)\cos\left(\frac{n\pi y}{L}\right) \tag{21c}$$

By the substitution of Eq. (22) in the constitutive equations of different nonlocal plate theories and solving the obtained eigenvalue problems, critical axial buckling loads of SLGSs embedded in elastic media are achieved as:

For CLPT

$$\begin{aligned}P_{CLPT} = &-(3L^4 k_w - 3L^4 K_w v^2 + 12\pi^4 k_s m^4 \mu \\ &+ E\pi^4 h^3 m^4 + 6L^2 \pi^2 k_s m^2 + 6L^2 \pi^2 k_w m^2 \mu \\ &- 12\pi^4 k_s m^4 \mu v^2 - 6L^2 \pi^2 k_s m^2 v^2 \\ &- 6L^2 \pi^2 k_w m^2 \mu v^2)/ \\ &6\pi^2 m^2 (L^2 + 2\pi^2 \mu m^2)(v-1)(v+1)\end{aligned} \tag{22}$$

For FSDT

$$\begin{aligned}P_{FSDT} = &(6G\kappa L^6 k_w - 6G\kappa L^6 k_w v^2 + 12GL^4 \pi^2 \kappa k_s m^2 \\ &+ 4E\pi^6 h^2 k_s m^6 \mu + 2EL^2 \pi^4 h^2 k_w m^2 \\ &+ 24GL^2 \pi^4 \kappa k_s m^4 \mu + 12GL^4 \pi^2 \kappa k_w m^2 \mu \\ &+ 2EGL^2 \pi^4 h^3 \kappa m^4 + 2EL^2 \pi^4 h^2 k_w m^4 \mu \\ &- 12GL^4 \pi^2 \kappa k_s m^2 v^2 - 24GL^2 \pi^4 \kappa k_s m^4 \mu v^2 \\ &- 12GL^4 \pi^2 \kappa k_w m^2 \mu v^2)/ \\ &(2\pi^2 m^2 (L^2 + 2\pi^2 \mu m^2) \\ &(-6G\kappa L^2 v^2 + 6G\kappa L^2 + E\pi^2 h^2 m^2))\end{aligned} \tag{23}$$

For HSDT

$$\begin{aligned}P_{HSDT} = &(-17640GL^6 k_w + 99E^2 \pi^6 h^5 m^6 \\ &- 35280GL^6 k_w v^2 + 17640GL^6 k_w v^4 \\ &+ 35280GL^4 \pi^2 k_s m^2 + 85E^2 \pi^6 h^5 m^6 v \\ &- 70560GL^4 \pi^2 k_s m^2 v^2 \\ &+ 35280GL^4 \pi^2 k_s m^2 v^4 \\ &+ 14280L^2 \pi^4 k_s m^4 \mu + 35280GL^4 \pi^2 k_w m^2 \mu \\ &+ 14280E\pi^6 h^2 k_s m^6 \mu + 6300EGL^2 \pi^4 h^3 m^4 \\ &+ 7140EL^2 \pi^4 k_s h^2 m^4 + 3570EL^4 \pi^2 k_w h^2 m^2 \\ &+ 420EGL^2 \pi^4 h^3 m^4 v + 7140EL^2 \pi^4 k_w h^2 m^4 \mu\end{aligned} \tag{24}$$

$$-141120GL^2\pi^4 k_s m^4 \mu v^2$$
$$+70560GL^2\pi^4 k_s m^4 \mu v^4$$
$$-70560GL^4\pi^2 k_w m^2 \mu v^2$$
$$-35280GL^4\pi^2 k_w m^2 \mu v^4 \tag{24}$$
$$-14280E\pi^6 h^2 k_s m^6 \mu v^2$$
$$-6300EGL^2\pi^4 h^3 m^4 v^2$$
$$-420EGL^2\pi^4 h^3 m^4 v^3$$

$$-7140EL^2\pi^4 k_s h^2 m^4 v^2$$
$$-3570EL^4\pi^2 k_w h^2 m^2 v^2$$
$$-7140EL^2\pi^4 k_w h^2 m^4 \mu v^2)/ \tag{24}$$
$$(420\pi^2 m^2 (L^2 + 2\pi^2 \mu m^2)(v-1)(v+1)$$
$$-84GL^2 v^2 + 84GL^2 + 17E\pi^2 h^2 m^2))$$

It should be noted that the above explicit expressions were obtained by assuming $m = n$.

Table 1 Axial buckling loads for the first buckling mode

L/h	μ	P_CLPT(nN) KW = 0 KS = 0	P_CLPT(nN) KW = 107 KS = 2×105	P_FSDT(nN) KW = 0 KS = 0	P_FSDT(nN) KW = 107 KS = 2×105	P_HSDT(nN) KW = 0 KS = 0	P_HSDT(nN) KW = 107 KS = 2×105
	0	5.7397	5.7458	5.4821	5.4881	5.9578	5.9638
	0.5	3.0962	3.1023	2.9572	2.9633	3.2139	3.2199
	1	2.1199	2.1260	2.0247	2.0308	2.2004	2.2065
	1.5	1.6117	1.6177	1.5393	1.5454	1.6729	1.6790
10	2	1.3000	1.3061	1.2417	1.2477	1.3494	1.3555
	2.5	1.0894	1.0954	1.0405	1.0465	1.1308	1.1368
	3	0.9375	0.9435	0.8954	0.9014	0.9731	0.9791
	3.5	0.8227	0.8288	0.7858	0.7919	0.8540	0.8600
	4	0.7330	0.7391	0.7001	0.7062	0.7609	0.7669
	0	1.4349	1.4586	1.4183	1.4419	1.5372	1.5608
	0.5	1.1825	1.2062	1.1688	1.1924	1.2668	1.2904
	1	1.0056	1.0293	0.9940	1.0176	1.0773	1.1009
	1.5	0.8748	0.8984	0.8646	0.8882	0.9371	0.9607
20	2	0.7741	0.7977	0.7651	0.7887	0.8292	0.8528
	2.5	0.6941	0.7178	0.6861	0.7097	0.7436	0.7672
	3	0.6292	0.6528	0.6219	0.6455	0.6740	0.6976
	3.5	0.5753	0.5990	0.5686	0.5923	0.6163	0.6399
	4	0.5300	0.5536	0.5238	0.5474	0.5677	0.5914
	0	0.6377	0.6907	0.6344	0.6873	0.6873	0.7402
	0.5	0.5825	0.6354	0.5795	0.6324	0.6277	0.6806
	1	0.5360	0.5890	0.5333	0.5862	0.5777	0.6306
	1.5	0.4965	0.5494	0.4939	0.5468	0.5350	0.5879
30	2	0.4623	0.5152	0.4599	0.5128	0.4982	0.5511
	2.5	0.4326	0.4855	0.4303	0.4832	0.4662	0.5191
	3	0.4064	0.4593	0.4043	0.4572	0.4380	0.4909
	3.5	0.3833	0.4362	0.3813	0.4342	0.4130	0.4659
	4	0.3626	0.4155	0.3607	0.4136	0.3907	0.4436
	0	0.3587	0.4526	0.3577	0.4516	0.3874	0.4813
	0.5	0.3406	0.4345	0.3396	0.4335	0.3678	0.4617
	1	0.3241	0.4180	0.3232	0.4171	0.3500	0.4439
	1.5	0.3092	0.4031	0.3083	0.4022	0.3339	0.4278
40	2	0.2956	0.3895	0.2948	0.3887	0.3193	0.4132
	2.5	0.2832	0.3771	0.2823	0.3763	0.3058	0.3997
	3	0.2717	0.3656	0.2709	0.3648	0.2935	0.3874
	3.5	0.2612	0.3551	0.2604	0.3543	0.2821	0.3760
	4	0.2514	0.3453	0.2507	0.3446	0.2715	0.3654

5. Results and discussion

5.1 Validation

In this section, we give the selected numerical results for the analytical solutions provided in the previous section. For validation, we assume the following properties for SLGSs: $v = 0.16$, $E = 1$ TPa, $h = 0.34$ nm and the side length (L) of the square SLGSs range between $\frac{L}{h} = 10$ and 40 (Pradhan *et al*. 2010). These results are compared with those reported by Pradhan *et al*. (2010) for buckling and is shown in Fig. 3. The results are perfectly matched. Because, unlike reference, graphene is placed on an elastic medium, we use $k_s = 0$ and $k_w = 0$.

5.2 Effect of various parameters on critical buckling load

Axial buckling load values of SLGSs for the first three buckling modes are summarized in Tables 1-3. By increasing the values of nonlocal parameter and aspect
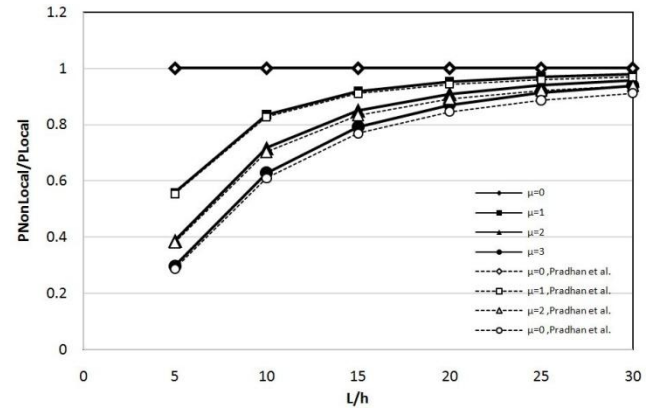

Fig. 3 Comparison and validation of the proposed model with Pradhan and Murmu model

ratio, buckling load decreases but by increasing mode number, it increases. This is more significant for lower aspect ratios and higher mode numbers. Furthermore, it is observed that by introducing the effect of transverse shear

Table 2 Axial buckling loads for the second buckling mode

L/h	μ	P_CLPT(nN) KW = 0 KS = 0	P_CLPT(nN) KW = 107 KS = 2×105	P_FSDT(nN) KW = 0 KS = 0	P_FSDT(nN) KW = 107 KS = 2×105	P_HSDT(nN) KW = 0 KS = 0	P_HSDT(nN) KW = 107 KS = 2×105
	0	22.9588	22.9605	19.3258	19.3274	21.2349	21.2366
	0.5	5.2001	5.2018	4.3772	4.3789	7.8096	4.8113
	1	2.9321	2.9338	2.4681	2.4698	2.7119	2.7136
	1.5	2.0416	2.0433	1.7186	1.7202	1.8883	1.88900
10	2	1.5661	1.5677	1.3182	1.3199	1.4485	1.4501
	2.5	1.2702	1.2718	1.0692	1.0708	1.1748	1.1765
	3	1.0683	1.0700	0.8993	0.9009	0.9881	0.9898
	3.5	0.9218	0.9235	0.7760	0.7776	0.8526	0.8543
	4	0.8107	0.8123	0.6824	0.6841	0.7498	0.7515
	0	5.7397	5.7458	5.4821	5.4881	5.9578	5.9638
	0.5	3.0962	3.1023	2.9572	2.9633	3.2139	3.2199
	1	2.1199	2.1260	2.0247	2.0308	2.2004	2.2065
	1.5	1.6117	1.5393	1.5393	1.5454	1.6729	1.6790
20	2	1.3000	1.3061	1.2417	1.2477	1.3494	1.3555
	2.5	1.0894	1.0954	1.0405	1.0465	1.1308	1.1368
	3	0.9375	0.9435	0.8954	0.9014	0.9731	0.9791
	3.5	0.8227	0.8288	0.7858	0.7919	0.8540	0.8600
	4	0.7330	0.7391	0.7001	0.7062	0.7609	0.7669
	0	2.5510	2.5644	2.4988	2.5122	2.7102	2.7235
	0.5	1.8493	1.8626	1.8114	1.8248	1.9647	1.9780
	1	1.4503	1.4637	1.4206	1.4340	1.5408	1.5542
	1.5	1.1930	1.2063	1.1686	1.1819	1.2674	1.2808
30	2	1.0132	0.0265	0.9924	1.0058	1.0764	1.0898
	2.5	0.8805	0.8939	0.8625	0.8758	0.9354	0.9488
	3	0.7785	0.7919	0.7626	0.7760	0.8271	0.8405
	3.5	0.6977	0.7111	0.6834	0.6968	0.7413	0.7546
	4	0.6321	0.6455	0.6192	0.6326	0.6716	0.6849

Table 2 Continued

L/h	μ	P_CLPT(nN) KW = 0 KS = 0	P_CLPT(nN) KW = 107 KS = 2×105	P_FSDT(nN) KW = 0 KS = 0	P_FSDT(nN) KW = 107 KS = 2×105	P_HSDT(nN) KW = 0 KS = 0	P_HSDT(nN) KW = 107 KS = 2×105
	0	1.4349	1.4586	0.4183	1.4419	1.5372	1.5608
	0.5	1.1825	1.2062	1.1688	1.1924	1.2668	1.2904
	1	1.0056	1.0293	0.9940	1.0176	1.0773	1.1009
	1.5	0.8748	0.8984	0.8646	0.8882	0.9371	0.9607
40	2	0.7741	0.7977	0.7651	0.7887	0.8292	0.8528
	2.5	0.6941	0.7178	0.6861	0.7097	0.7436	0.7672
	3	0.6292	0.6528	0.6219	0.6455	0.6740	0.6973
	3.5	0.5753	0.5990	0.5686	0.5923	0.6163	0.6399
	4	0.5300	0.5536	0.5238	0.5474	0.5677	0.5914

stress into FSDT and HSDT, axial buckling load values are decreased for all nonlocal parameter values and this decrease is more significant for lower aspect ratios and higher mode numbers.

It is found that by increasing the values of both aspect ratio and nonlocal parameter, the difference between the

Table 3 Axial buckling loads for the second buckling mode

L/h	μ	P_CLPT(nN) KW = 0 KS = 0	P_CLPT(nN) KW = 107 KS = 2×105	P_FSDT(nN) KW = 0 KS = 0	P_FSDT(nN) KW = 107 KS = 2×105	P_HSDT(nN) KW = 0 KS = 0	P_HSDT(nN) KW = 107 KS = 2×105
	0	51.6574	51.6583	36.3022	36.303	40.6365	40.6374
	0.5	5.9486	5.9495	4.1804	4.1812	4.6795	4.6804
	1	3.156	3.1569	2.2179	2.2187	2.4827	2.4835
	1.5	2.1478	2.1486	1.5093	1.5102	1.6895	1.6904
10	2	1.6277	1.6286	1.1439	1.1447	1.2805	1.2813
	2.5	1.3104	1.3113	0.9209	0.9218	1.0309	1.0317
	3	1.0967	1.0975	0.7707	0.7715	0.8627	0.8636
	3.5	0.9429	0.9437	0.6626	0.6634	0.7417	0.7426
	4	0.8269	0.8277	0.5811	0.582	0.6505	0.6513
	0	12.9144	12.9172	11.6793	11.6821	12.7508	12.7536
	0.5	4.4212	4.424	3.9984	4.0012	4.3652	4.368
	1	2.6672	2.67	2.4121	2.4149	2.6334	2.6362
	1.5	1.9096	1.9124	1.727	1.7298	1.8854	1.8882
20	2	1.4872	1.49	1.3449	1.3477	1.4683	1.4711
	2.5	1.2178	1.2206	1.1013	1.1041	1.2023	1.2051
	3	1.031	1.0338	0.9324	0.9352	1.018	1.0208
	3.5	0.8939	0.8967	0.8084	0.8112	0.8826	0.8854
	4	0.789	0.7918	0.7136	0.7164	0.779	0.7818
	0	5.7397	5.7458	5.4821	5.4881	5.9578	5.9638
	0.5	3.0962	3.1023	2.9572	2.9633	3.2139	3.2199
	1	2.1199	2.126	2.0247	2.0308	2.2004	2.2065
	1.5	1.6117	1.6177	1.5393	1.5454	1.6729	1.679
30	2	1.3	1.3061	1.2417	1.2477	1.3494	1.3555
	2.5	1.0894	1.0954	1.0405	1.0465	1.1308	1.1368
	3	0.9375	0.9435	0.8954	0.9014	0.9731	0.9791
	3.5	0.8227	0.8288	0.7858	0.7919	0.854	0.86
	4	0.733	0.7391	0.7001	0.7062	0.7609	0.7669

Table 3 Continued

L/h	μ	P_CLPT(nN) KW = 0 KS = 0	P_CLPT(nN) KW = 107 KS = 2×105	P_FSDT(nN) KW = 0 KS = 0	P_FSDT(nN) KW = 107 KS = 2×105	P_HSDT(nN) KW = 0 KS = 0	P_HSDT(nN) KW = 107 KS = 2×105
	0	3.2286	3.2392	3.1454	3.156	3.413	3.4236
	0.5	2.1811	2.1917	2.1249	2.1356	2.3057	2.3163
	1	1.6468	1.6574	1.6044	1.615	1.7409	1.7515
	1.5	1.3228	1.3334	1.2887	1.2993	1.3983	1.4089
40	2	1.1053	1.1159	1.0768	1.0875	1.1684	1.179
	2.5	0.9492	0.9599	0.9248	0.9354	1.0035	1.0141
	3	0.8318	0.8424	0.8104	0.821	0.8793	0.8899
	3.5	0.7402	0.7508	0.7211	0.7318	0.7825	0.7931
	4	0.6668	0.6774	0.6496	0.6602	0.7049	0.7155

predicted values of critical axial buckling load obtained from Winkler and Pasternak foundation models is also increased. In addition, it is observed that all nonlocal plate theories have almost similar patterns, especially regarding the variations of aspect ratio.

In this work, we investigate the axial buckling behavior of SLGSs embedded in elastic media. Winkler and Pasternak foundation models are employed for the simulation of surrounding elastic media. To consider small-scale effect on buckling, Eringen's nonlocal continuum elasticity is employed in different plate theories including CLPT, FSDT, and HSDT. Exact solutions are obtained for SLGSs with simply supported boundary conditions. Explicit equations are obtained to calculate the axial buckling loads of SLGSs for different nonlocal plate theories.

According to our findings, considering elastic foundation increases axial buckling loads for all nonlocal parameter values, which is more significant at higher aspect ratios for all mode numbers. In addition, we find that, nonlocality has the strongest effect on FSDT among all nonlocal plate theories, especially for a specific range of nonlocal parameter values.

In addition, we conclude that the critical axial buckling load of embedded SLGSs simulated by Pasternak foundation model is relatively higher than those simulated by Winkler foundation model this difference is almost constant for all nonlocal plate theories, especially in the case of the variation of aspect ratio and is more significant at higher aspect ratio and nonlocal parameter values.

References

Alizadeh, M. and Fattahi, A.M. (2019), "Non-classical plate model for FGMs", *Eng. Comput.*, **35**(1), 215-228.

Azizi, S., Safaei, B., Fattahi, A.M. and Tekere, M. (2015), "Nonlinear vibrational analysis of nanobeams embedded in an elastic medium including surface stress effects", *Adv. Mater. Sci. Eng.*, **2015**, 1-7. http://dx.doi.org/10.1155/2015/318539

Behfar, K. and Naghdabadi, R. (2005), "Nanoscale vibrational analysis of a multi-layered graphene sheet embedded in an elastic medium", *Compos. Sci. Technol.*, **65**(7), 1159-1164. https://doi.org/10.1016/j.compscitech.2004.11.011

Bouadi, A., Bousahla, A.A., Houari, M.S.A., Heireche, H. and Tounsi, A. (2018), "A new nonlocal HSDT for analysis of stability of single layer graphene sheet", *Adv. Nano Res., Int. J.*, **6**(2), 147-162. https://doi.org/10.12989/anr.2018.6.2.147

Daouadji, T.H. and Adim, B. (2017), "Mechanical behaviour of FGM sandwich plates using a quasi-3D higher order shear and normal deformation theory", *Struct. Eng. Mech., Int. J.*, **61**(1), 49-63. https://doi.org/10.12989/sem.2018.67.2.143

Ebrahimi, F. and Barati, M.R. (2018), "Surface and flexoelectricity effects on size-dependent thermal stability analysis of smart piezoelectric nanoplates", *Struct. Eng. Mech., Int. J.*, **67**(2), 143-153. https://doi.org/10.12989/sem.2017.61.1.049

Eringen, A.C. (1972), "Linear theory of nonlocal elasticity and dispersion of plane waves", *Int. J. Eng. Sci.*, **10**(5), 425-435. https://doi.org/10.1016/0020-7225(72)90050-X

Fattahi, A.M. and Safaei, B. (2017), "Buckling analysis of CNT-reinforced beams with arbitrary boundary conditions", *Microsyst. Technol.*, **23**(10), 5079-5091. https://doi.org/10.1007/s00542-017-3345-5

Fattahi, A.M. and Sahmani, S. (2017), "Size dependency in the axial postbuckling behavior of nanopanels made of functionally graded material considering surface elasticity", *Arab. J. Sci. Eng.*, **42**, 4617-4633. https://doi.org/10.1007/s13369-017-2600-5

Filiz, S. and Aydogdu, M. (2010), "Axial vibration of carbon nanotube heterojunctions using nonlocal elasticity", *Compos. Mater. Sci.*, **49**(3), 619-627. https://doi.org/10.1016/j.commatsci.2010.06.003

Hao, M.J., Guo, X.M. and Wang, Q. (2010), "Small-scale effect on torsional buckling of multi-walled carbon nanotubes", *Eur. J. Mech. A/Solids*, **29**(1), 49-55. https://doi.org/10.1016/j.euromechsol.2009.05.008

Jalali, M.H., Zargar, O. and Baghani, M. (2018), "Size-dependent vibration analysis of FG microbeams in thermal environment based on modified couple stress theory", *IJST-T Mech. Eng.*, 1-11. https://doi.org/10.1007/s40997-018-0193-6

Kiani, K. (2010), "A meshless approach for free transverse vibration of embedded single-walled nanotubes with arbitrary boundary conditions accounting for nonlocal effect", *Int. J. Mech. Sci.*, **52**(10), 1343-1356. https://doi.org/10.1016/j.ijmecsci.2010.06.010

Kitipornchai, S., He, X.Q. and Liew, K.M. (2005), "Continuum model for the vibration of multilayered graphene sheets", *Phys. Rev. B*, **72**(7), 075443.

Liew, K.M., He, X.Q. and Kitipornchai, S. (2006), "Predicting nanovibration of multi-layered graphene sheets embedded in an elastic matrix", *Acta Mater.*, **54**(16), 4229-4236. https://doi.org/10.1016/j.actamat.2006.05.016

Mohammadsalehi, M., Zargar, O. and Baghani, M. (2017), "Study of non-uniform viscoelastic nanoplates vibration based on nonlocal first-order shear deformation theory", *Meccanica*, **52**(4-5), 1063-1077. https://doi.org/10.1007/s11012-016-0432-0

Moheimani, R. and Ahmadian, M.T. (2012), "On Free Vibration of Functionally Graded Euler-Bernoulli Beam Models Based on the Non-Local Theory", *ASME 2012 International Mechanical Engineering Congress and Exposition*, **12**, Vibration Acoustics and Wave Propagation, Houston, TX, USA, November.

Moradi-Dastjerdi, R. and Momeni-Khabisi, H. (2016), "Dynamic analysis of functionally graded nanocomposite plates reinforced by wavy carbon nanotube", *Steel Compos. Struct., Int. J.*, **22**(2), 277-299. https://doi.org/10.12989/scs.2016.22.2.277

Moradi-Dastjerdi, R. and Malek-Mohammadi, H. (2017), "Biaxial buckling analysis of functionally graded nanocomposite sandwich plates reinforced by aggregated carbon nanotube using improved high-order theory", *J. Sandw. Struct. Mater.*, **19**, 736-769. https://doi.org/10.1177/1099636216643425

Moradi-Dastjerdi, R., Malek-Mohammadi, H. and Momeni-Khabisi, H. (2017), "Free vibration analysis of nanocomposite sandwich plates reinforced with CNT aggregates", *ZAMM – J. Appl. Math. Mech./Zeitschrift Fur Angew Math Und Mech*, **97**, 1418-1435. https://doi.org/10.1002/zamm.201600209

Pasharavesh, A., Vaghasloo, Y.A., Ahmadian, M.T. and Moheimani, R. (2011), "Nonlinear vibration analysis of nano to micron scale beams under electric force using nonlocal theory", *ASME Conference Proceedings*, *DETC2011-47615*, 145-151, Washington, DC, USA, August.

Pasternak, P.L. (1954), "On a New Method of Analysis of an Elastic Foundation by Means of Two Foundation Constants", *Gosudarstvennoe Izdatelstro Liberaturi po Stroitelstvui Arkhitekture*, Moscow, Russia.

Peddieson, J., Buchanan, G.R. and McNitt, R.P. (2003), "Application of nonlocal continuum models to nanotechnology", *Int. J. Eng. Sci.*, **41**(3), 305-312. https://doi.org/10.1016/S0020-7225(02)00210-0

Pradhan, S.C. and Murmu, T. (2009), "Small scale effect on vibration of embedded multilayered graphene sheets based on nonlocal continuum models", *Phys. Lett. A*, **373**(11), 1062-1069. https://doi.org/10.1016/j.physleta.2009.01.030

Pradhan, S.C. and Murmu, T. (2010), "Small scale effect on the buckling analysis of single-layered graphene sheet embedded in an elastic medium based on nonlocal plate theory", *Physica E*, **42**(5), 1293-1301. https://doi.org/10.1016/j.physe.2009.10.053

Qin, Z., Pang, X., Safaei, B. and Chu, F. (2019), "Free vibration analysis of rotating functionally graded CNT reinforced composite cylindrical shells with arbitrary boundary conditions", *Compos. Struct.*, **220**, 847-860. https://doi.org/10.1016/j.compstruct.2019.04.046

Safaei, B. and Fattahi, A.M. (2017), "Free vibrational response of single-layered graphene sheets embedded in an elastic matrix using different nonlocal plate models", *Mechanika*, **23**(5), 678-687. https://doi.org/10.5755/j01.mech.23.5.14883

Safaei, B., Naseradinmousavi, P. and Rahmani, A. (2016), "Development of an accurate molecular mechanics model for buckling behavior of multi-walled carbon nanotubes under axial compression", *J. Mol. Graph. Modell.*, **65**, 43-60. https://doi.org/10.1016/j.jmgm.2016.02.001

Safaei, B., Moradi-Dastjerdi, R., Qin, Z. and Chu, F. (2019), "Frequency-dependent forced vibration analysis of nanocomposite sandwich plate under thermo-mechanical loads", *Compos. Part B Eng.*, **161**, 44-54. https://doi.org/10.1016/j.compositesb.2018.10.049

Sahmani, S. and Fattahi, A.M. (2017a), "An anisotropic calibrated nonlocal plate model for biaxial instability analysis of 3D metallic carbon nanosheets using molecular dynamics simulations", *Mater. Res. Express*, **4**(6), 1-14.

Sahmani, S. and Fattahi, A.M. (2017b), "Calibration of developed nonlocal anisotropic shear deformable plate model for uniaxial instability of 3D metallic carbon nanosheets using MD simulations", *Comput. Method Appl. Mech. Eng.*, **322**, 187-207. https://doi.org/10.1016/j.cma.2017.04.015

Shahriari, B., Zargar, O., Baghani, M. and Baniassadi, M. (2018), "Free vibration analysis of rotating functionally graded annular disc of variable thickness using generalized differential quadrature method", *Scientia Iranica*, **25**(2), 728-740. https://doi.org/10.24200/SCI.2017.4325

Shen, H.S. (2010), "Buckling and postbuckling of radially loaded microtubules by nonlocal shear deformable shell model", *J. Theor. Biol.*, **264**(2), 386-394. https://doi.org/10.1016/j.jtbi.2010.02.014

Shen, L., Shen, H.S. and Zhang, C.L. (2010), "Nonlocal plate Model for Nonlinear Vibration of Single Layer Graphene Sheets in Thermal Enviroments", *Compos. Mater. Sci.*, **48**(3), 680-685. https://doi.org/10.1016/j.commatsci.2010.03.006

Winkler, E. (1867), "Theory of Elasticity and Strength", H. Dominicus, Prague, Czech Republic.

Yang, J., Ke, L.L. and Kitipornchai, S. (2010), "Nonlinear free vibration of single-walled carbon nanotubes using nonlocal Timoshenko beam theory", *Physica E*, **42**(5), 1727-1735. https://doi.org/10.1016/j.physe.2010.01.035

Zenkour, A.M. (2018), "Nonlocal elasticity and shear deformation effects on thermal buckling of a CNT embedded in a viscoelastic medium", *Eur. Phys. J. Plus*, **133**, 193. https://doi.org/10.1140/epjp/i2018-12014-2

CC